

Viscous Fingering Fractals in Porous Media

Knut Jørgen Måløy, Jens Feder, and Torstein Jøssang

Institute of Physics, University of Oslo, Blindern, 0316 Oslo 3, Norway

(Received 12 July 1985)

Gas displacing a high-viscosity fluid in a two-dimensional porous disk intrudes in the form of ramified fingers similar to the structures obtained in diffusion-limited aggregation. We find that the resulting finger structures are described by a fractal dimension $D = 1.62 \pm 0.04$ consistent with D for diffusion-limited aggregation clusters. This result confirms the analogy between diffusion-limited aggregation and two-fluid displacement in porous media introduced by Paterson.

PACS numbers: 47.55.Mh, 05.40.+j, 47.55.Kf

Viscous fingering in porous media has been extensively studied in the past and has recently become a field of very active research. The phenomenon is also of practical importance in the recovery of oil.

When a fluid displaces another fluid with a higher viscosity the interface is unstable and the driving fluid intrudes into the viscous fluid in the form of "fingers." Saffman and Taylor¹ developed the theory of viscous fingering for situations where the fluids are immiscible and where the flow is described by Darcy's law valid in porous media for each of the fluids separately. This theory also describes the flow of ordinary fluids in the two-dimensional (2D) geometry given in Hele-Shaw² cells consisting of two parallel glass plates separated by a very small gap a . Saffman and Taylor verified their theory by experiments on rectangular Hele-Shaw cells and found that a single viscous finger developed with a width that decreased to half the channel width as the capillary number $N_{ca} = U\mu/\sigma$ increases above 0.04. Here U is the fingertip velocity, μ is the viscosity of the high-viscosity fluid, and σ is the interfacial tension.

Paterson³ studied 2D radial fingering in circular Hele-Shaw cells and concluded that when the circumference of the bubble injected at the center increased beyond a critical value $\lambda_c/a \approx N_{ca}^{-1/2}$, it became unstable and developed fingers with a width of the order of λ_c . As the bubble grew further the fingers bifurcated when their width increased beyond $2\lambda_c$.

We study radial displacement of *immiscible* fluids in a 2D *random porous medium*, and observe a fingering structure dramatically different from Hele-Shaw cell fingers at comparable N_{ca} ; see Fig. 1. Instead of the smooth broad fingers observed in the Hele-Shaw cells, we find that the fingering process produces ramified fractal⁴ structures with a fractal dimension $D = 1.62 \pm 0.04$, consistent with the diffusion-limited aggregation (DLA) model discussed below.

Our results at high N_{ca} extend the recent experiments by Lenormand and Zarcone⁵ from the invasion percolation to the DLA regime. They studied linear displacement in a 2D porous medium consisting of

etched channels on a square lattice at extremely low capillary numbers $N_{ca} < 10^{-6}$. The injected fluid forms a ramified structure with a fractal dimension D in the range 1.80 to 1.83 in agreement with the invasion percolation model with trapping.⁶

Recently Nittmann, Daccord, and Stanley⁷ studied 2D viscous fingering of *miscible* fluids in a Hele-Shaw channel. By choosing a high-molecular-mass polysaccharide aqueous solution as the viscous fluid and water as the driving fluid, they eliminate the interfacial tension and obtain high effective N_{ca} . However, the solution is non-Newtonian and exhibits shear thinning. N_{ca} is therefore not well defined. The observed fingering structure is fractal with $D = 1.39$, and below the DLA

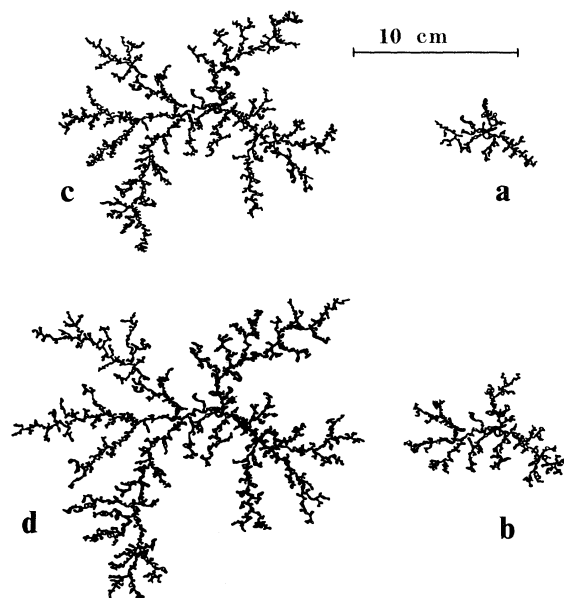


FIG. 1. Fingers of air displacing liquid epoxy in a 2D porous medium consisting of 1.6-mm-diam glass spheres in a monolayer 40 cm in diameter at $N_{ca} = 0.04$. The center of injection is at the circle near the center of the structure. (a) $t = 2$ s after the start of injection; (b) $t = 3.9$ s; (c) $t = 17.2$ s; (d) $t = 19.1$ s.

result⁸⁻¹⁰ 1.68. In their linear displacement the lateral channel width W controls the fingering, and $D \rightarrow 1$ when the finger length is $\gg W$.

There have been several studies of 3D viscous fingering in porous media in packs of sand,¹¹ in transparent models made of glass powder,^{12,13} and in consolidated transparent models.^{14,15} These studies show that 3D viscous fingering also generates ramified structures. However, they have so far not been analyzed in terms of their fractal structure. Also note that gravity effects cannot be ignored in 3D systems.

Paterson¹⁶ pointed out the analogy between two-fluid flow in porous media and the DLA process.¹⁷ Darcy's law states that in a porous medium the fluid flux U is proportional to the gradient of the pressure p :

$$U = -(k/\mu)\nabla p. \quad (1)$$

The permeability, k , is characteristic of the porous material. For the Hele-Shaw cell with plate separation a , Eq. (1) applies with $k = a^2/12$. For incompressible fluids $\nabla \cdot U = 0$, and Eq. (1) leads to the Laplace equation for the pressure,

$$\nabla^2 p = 0, \quad (2)$$

Consider a disk of radius R_0 , and assume that the viscosity of the fluid injected at the center is negligible compared with the viscosity μ of the fluid being displaced. Then the pressure everywhere in the growing bubble is p_i , whereas the pressure at the rim of a circular system is p_0 . The pressure in the fluid being driven is given by Eq. (2), and equals p_i at the interface if the interfacial tension may be ignored, i.e., for large $N_{ca} = U\mu/\sigma$. The interface moves with a velocity given by Eq. (1).

This fluid displacement is analogous¹⁶ to DLA,^{8-10,17} where "particles" that walk at random stick irreversibly on contact with the growing cluster. The number of particles or mass $N(r)$ within a radius r from the seed particle has the form $N(r) \sim r^D$, where the fractal dimension⁴ is^{8,9} $D = 1.68 \pm 0.05$ for 2D systems. In a continuum description with a steady flux of walkers from a rim far away from the seed, the probability $p(r,t)$ that a walker is at a point r at time t satisfies^{8,17} Eq. (2), with the condition $p = 0$ at the boundary of the aggregate and $p = 1$ at the rim. The cluster boundary moves with a velocity proportional to ∇p , and Eq. (1) is satisfied for DLA as well.

In order to test these ideas we made 2D porous systems by coating a 40 cm-diam disk of 6-mm-thick Plexiglas with a 0.1-mm layer of epoxy, and spread a layer of glass spheres with diameter 1.0 or 1.6 mm onto the disk. After the epoxy has hardened the excess glass spheres are removed leaving a monolayer of spheres. This disk is glued onto another Plexiglas disk with Ciba-Geigy epoxy XW 396 with hardener UP XW 397. The resulting system has a porosity of about

0.45. The cell is filled by injecting glycerol or epoxy through a hole at the center. We used epoxy so that the resulting fractal is preserved when the epoxy hardens (gel time 6–10 h, hard after 24 h). The experiments are performed by injection of air at a fixed pressure of typically 20 mbar above the pressure at the rim. The resulting finger structure is photographed at a maximum rate of a picture every 1.9 s, and the experiment takes about 25 s. The viscosity of the epoxy is constant during the experiment. In the photographs the individual spheres and the meniscus separating the two fluids is clearly visible. We trace the invading fingers on a transparency placed over the picture, using India ink. These tracings are digitized with use of an RCA TC2055CX camera and a Tecmar Video van Gogh interface in an IBM PC.

Figure 1 shows a sequence of pictures of the displacement of freshly mixed epoxy by air at $N_{ca} \approx 0.04$. Experiments with glycerol, $N_{ca} = 0.15$, generated fingering structures that cannot be distinguished from those in Fig. 1. These fingering structures are very similar to pictures of 2D DLA aggregates found in the literature.⁸⁻¹⁰ They are treelike in structure, showing no loops. The fingers are narrow and only occasionally surround several spheres. By closer inspection one finds that only the outer fingers grow, the others are screened, as is the case for the growth of DLA clusters.

We analyze the viscous fingering structures by digitizing pictures as shown in Fig. 1 with a resolution of 256×256 pixels, and obtain a cluster of black pixels representing the fingering structure. We calculate the number $N(r)$ of black pixels as a function of the distance, r , from the center of injection. For fractal structures we expect $N(r)$ to have the form

$$N(r) = N_0(r/R_g)^D f(r/R_g). \quad (3)$$

Here R_g is a characteristic size of the fractal—we use the radius of gyration—and N_0 is the number of black pixels. The crossover function $f(x)$ is constant in the range $a/R_g < x < 1$, and tends to x^{-D} for $x > 1$, and we find $N(r) \rightarrow N_0$ for $r \gg R_g$ as we should.

In Fig. 2 we plot $\log[N(r)/N_0]$ as a function of $\log(r/R_g)$ for the structures shown in Fig. 1. We have also included the analysis of a fingering structure obtained in glycerol at $N_{ca} = 0.15$. We find a very satisfying data collapse: The fingering structures at various times for a given experiment, and from experiments with different fluids, all fall on a single curve when plotted as in Fig. 2. Equation (2) holds only as an average over many clusters, and the fluctuations in $N(r)$ for each realization of the random finger structure are expected. From fits to these results in the range $2a < r < R_g$, we find for the larger clusters (c to e in Fig. 2) a fractal dimension of viscous fingers in 2D porous media of $D = 1.62 \pm 0.04$, somewhat below but

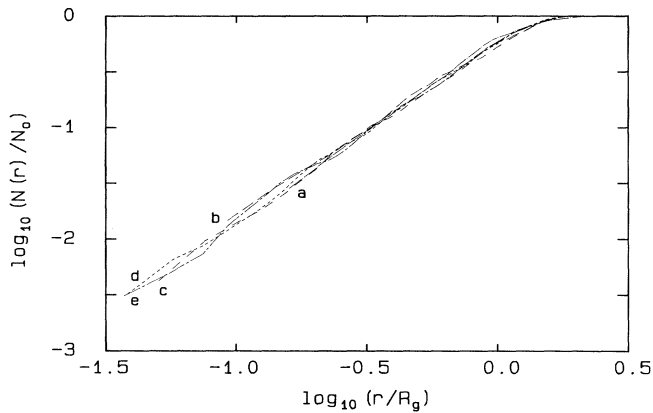


FIG. 2. The normalized finger structure volume $N(r)/N_0$ as function of the reduced radius r/R_g for the structures shown in Fig. 1. Curve *a*, $R_g=1.7$ cm; curve *b*, $R_g=2.9$ cm; curve *c*, $R_g=5.2$ cm; curve *d*, $R_g=6.6$ cm. Curve *e*, air displacing glycerol at $N_{ca}=0.15$, in a 40-cm disk of 1-mm spheres. $R_g=6.7$ cm.

consistent with the fractal dimension of the DLA clusters, and as expected well below the invasion percolation value $1.80 < D < 1.83$ found experimentally.⁵ The deviation from this power-law behavior of the finger structure is obtained by the plotting of the crossover function $f(r/R_g)$, from Eq. (3), with $D=1.62$, as shown in Fig. 3. Over more than a decade in r/R_g the fractal power-law behavior is observed before the finite size of the cluster makes $f(x)$ vanish. We have tested our analysis by digitizing the DLA cluster in Fig. 1 of Ref. 10. We find $D_{DLA}=1.65$, and similar fluctuations for $f(x)$ as shown in Fig. 3. The use of different origins near the center of injection for the evaluation of $N(r)$ gives results consistent with Fig. 2. However, since DLA clusters scale differently in the radial and tangential directions, we do not average over the whole fractal. A rough estimate of the fractal dimension can also be determined by counting the number $n(l) \sim l^{-D}$ of squares of side l needed to cover the fractal. This method gives D in the range 1.55 to 1.8, and does not allow for the crossover to finite cluster size at R_g , nor does the method allow for the radial/tangential anisotropy. In addition we find that the measurement of $N(r)$ gives a more robust estimate of D , in the sense that the estimates of D scatter less when the origin location, discriminator level, etc., is changed. We conclude that D is best determined from $N(r)$.

The dynamics of the fingering process is shown in Fig. 4. The distance r_m from the center of injection to the tip of the longest finger is plotted as function of t/t_0 , where t_0 is the breakthrough time when $r_m=R_0$. Two experiments on the same cell with glycerol, and one with epoxy, are shown. The points corresponding

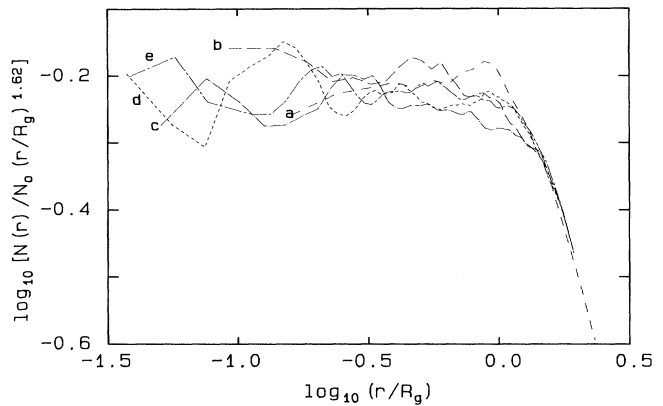


FIG. 3. Scaling plot of the results in Fig. 2. The crossover function $f(r/R_g) = N(r)/N_0(r/R_g)^D$ as function of r/R_g with $D=1.62$, for the structures shown in Fig. 1, and with parameters for epoxy (curves *a-d*) and glycerol (curve *e*) given in Figs. 1 and 2.

to the structures in Fig. 1 are marked. For a circular bubble of radius r at a fixed pressure p_i expanding into the viscous fluid, Eqs. (1) and (2) give the relation

$$t/t_0 \sim (r/R_0)^2 [1 - \ln(r/R_0)^2]. \tag{4}$$

This gives the fully drawn curve in Fig. 4, and it describes the data well. This indicates that the longest fingers control the potential flow and generate a “Faraday cage” with a radius almost equal to r_m screening the internal structure of shorter fingers. Matsushita *et al.*¹⁸ studied the fractal structure of 2D zinc metal leaves grown by electrodeposition and obtained $D=1.66 \pm 0.03$. They proposed that the ex-

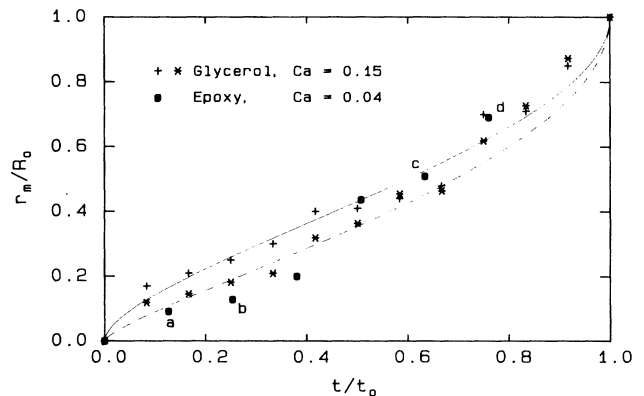


FIG. 4. The length r_m of the longest finger as function of time. Crosses and stars, two experiments on a 2D system of 1-mm glass spheres. Circles, results of experiment shown in Fig. 1, with points labeled correspondingly. “Ca” denotes N_{ca} . The curves are discussed in the text.

ponent 2 in Eq. (4) be replaced by D in order to account for the fact that less of the fluid is displaced by fractals than by bubbles. This replacement gives the dashed curve in Fig. 4. Our results do not allow a clear distinction between these two types of behavior. With new equipment that allows pictures at a higher rate we will investigate the time dependence in detail.

We conclude that viscous fingers form fractal structures with a fractal dimension $D = 1.62 \pm 0.04$, at high N_{ca} in a 2D porous medium. The finger structures are similar to 2D DLA clusters. They have the same fractal dimension and have a treelike structure with very few loops.

In the high- N_{ca} regime we have studied, the fluid interface advances on the pore level by at each instant selecting the most favorable pore. But in contrast to the invasion percolation limit⁵ $N_{ca} \ll 1$, the probability of entering a pore is not only determined by the width of the pore neck but also by the pressure gradient across it. The pressure gradient is, however, determined globally by the solution of the Laplace equation, and this fact is the source of the screening by the longest fingers. The dynamics of the finger growth is therefore controlled by the pressure distribution determined by the Laplace equation *and* by the discrete random advance on the pore level—it is this last step that is missed by continuum theories of two-phase fluid flow in porous media, and which is necessary for the analogy proposed by Paterson to hold. This interplay between the global field distribution and the discrete random propagation of the front leads to fractal finger structures also in dielectric breakdown.¹⁹

The use of Hele-Shaw cells to model viscous fingering in porous media must be reconsidered for *immiscible* fluids—since the fingering we observe is fractal in contrast with the observed^{1,3} finger structure in Hele-Shaw cells at comparable N_{ca} . It is an open question whether the radial Hele-Shaw fingers lead to a fractal structure or essentially fill the plane by repeated splitting in an infinite system. We believe that the experiments by Nittmann, Daccord, and Stanley⁷ in a Hele-Shaw channel may in fact model very high- N_{ca} flow in porous media and that the required randomness of the front dynamics is due to viscosity fluctuations in their viscous solution.

In summary, we have shown that viscous fingering at high N_{ca} is similar to DLA clusters being treelike in structure, having no loops and $D = 1.62$. This is substantially different from the invasion percolation limit $N_{ca} \ll 1$, observed by Lenormand and Zarcone,⁵ where the invaded pores form a fractal with loops of all sizes and with $D = 1.82$.

We thank Erling Pytte and Amnon Aharony for many stimulating and useful discussions. We are grateful to Statoil for a research grant, and one of us (K.J.M.) wishes to acknowledge the receipt of a fellowship from Statoil.

Note added.—After the submission of our paper, Lenormand²⁰ has estimated the various limits for invasion percolation, piston flow, and DLA fingering. He finds that if $N_{ca} > N_{ca}^* = (a/L)\mu_{air}/\mu$, then DLA fingering is expected. Using $a = 0.1$ cm, $L = 20$ cm, we find $N_{ca}^* = 10^{-6}$, and conclude that we have $N_{ca} \gg N_{ca}^*$.

¹P. G. Saffman and G. Taylor, Proc. Roy. Soc. London, Ser. A **245**, 312 (1958).

²H. S. S. Hele-Shaw, Nav. Archit. London Trans. Inst. **40**, 21 (1898).

³L. Paterson, J. Fluid Mech. **113**, 513 (1981).

⁴B. B. Mandelbrot, *The Fractal Geometry of Nature* (Freeman, San Francisco, 1982).

⁵R. Lenormand and C. Zarcone, Phys. Rev. Lett. **54**, 2226 (1985).

⁶D. Wilkinson, and J. F. Willemsen, J. Phys. A **16**, 3365 (1983).

⁷J. Nittmann, G. Daccord, and H. E. Stanley, Nature **314**, 141 (1985).

⁸T. A. Witten and L. M. Sander, Phys. Rev. Lett. **47**, 1400 (1981).

⁹P. Meakin, Phys. Rev. A **27**, 1495 (1983).

¹⁰T. A. Witten and Y. Kantor, Phys. Rev. B **30**, 4093 (1984).

¹¹W. F. Engelberts and L. J. Klinkenberg, in Proceedings of the Third World Petroleum Congress, 1951 (unpublished), Sec. 2, p. 544.

¹²P. van Meurs, Trans. Am. Inst. Min. Metall. Pet. Eng. **210**, 295 (1957).

¹³P. van Meurs and C. van der Poel, Trans. Am. Inst. Min. Metall. Pet. Eng. **213**, 103 (1958).

¹⁴B. Habermann, Trans. Metall. Soc. AIME **219**, 264 (1960).

¹⁵L. Paterson, V. Hornof, and G. Neale, Powder Technol. **33**, 265 (1982).

¹⁶L. Paterson, Phys. Rev. Lett. **52**, 1621 (1984).

¹⁷L. M. Sander, in *Scaling Phenomena in Disordered Systems*, edited by R. Pynn and A. Skjeltorp (Plenum, London, 1985); E. Guyon, *ibid.*

¹⁸M. Matsushita, M. Sano, Y. Hayakawa, H. Honjo, and Y. Sawada, Phys. Rev. Lett. **53**, 286 (1984).

¹⁹L. Niemeyer, L. Pietronero, and H. J. Wiesmann, Phys. Rev. Lett. **52**, 1033 (1984).

²⁰R. Lenormand, C. R. Acad. Sci. Ser. 2, **301**, 247 (1985).